Variation Characteristic of NDVI and its Response to Climate Change in the Middle and Upper Reaches of Yellow River Basin, China

Chengpeng Lu, *Member, IEEE*, Muchen Hou, Zhiliang Liu, Hengji Li, and Chenyu Lu

***Abstract*—Observing vegetation normalized difference vegetation index (NDVI) changes, climate change characteristics, and their response relationship have a great significance to the ecosystem's regulation and improvement the human settlements. Based on GIMMS AVHRR NDVI and MODIS NDVI datasets as well as temperature, precipitation, and sunshine duration data, this study used unitary linear trend analysis, correlation analysis, RS, and GIS data to analyze the spatiotemporal variation characteristics of vegetation NDVI in the middle and upper reaches of the Yellow River between 1989 and 2018. It also analyzed the spatiotemporal response between vegetation NDVI and climate factors (temperature, precipitation, and sunshine duration). The results showed that the vegetation NDVI in the study area had an increasing trend over the past 30 years, growing by 31.28%, and the NDVI change in 81.83% of the pixels was positive, the highest being 0.025. The temperature in the middle and upper reaches of the Yellow River showed an obvious upward trend, showing an overall distribution pattern of low temperature in the southwest and high temperature in the southeast. The precipitation showed a gentle upward trend and a spatial distribution pattern of a gradual decrease from southeast to northwest. The sunshine duration showed an obvious decreasing trend and a spatial distribution pattern of gradually increasing from southeast to northwest. In the past 30 years, the annual mean NDVI in the study area had a positive correlation with temperature and precipitation and a negative correlation with sunshine duration.**

***Index Terms*—Climate factor, human settlement environment, middle and upper reaches of the Yellow River, normalized difference vegetation index (NDVI), remote sensing.**

Manuscript received June 7, 2021; revised July 12, 2021; accepted August 15, 2021. Date of publication August 18, 2021; date of current version September 7, 2021. This work was supported in part by the National Natural Science Foundation of China under Grants 41701142 and 41971166, in part by the National Social Science Foundation and Projects of Marxist Theoretical Research and Construction under Grant 2020MYB070, and in part by the Fundamental Research Funds for the Central Universities under Grant 2020jbkyjc002. *(Corresponding author: Chengpeng Lu.)*

Chengpeng Lu was with the Key Lab of Pollution Ecology and Environmental Engineering, Institute of Applied Ecology, Chinese Academy of Sciences, Shenyang 110016, China. He is now with the Institute of County Economic Development and Rural Revitalization Strategy, School of Economics, Lanzhou University, Lanzhou 730000, China (e-mail: lcp@lzu.edu.cn).

Muchen Hou and Zhiliang Liu are with the Institute of County Economic Development and Rural Revitalization Strategy, School of Economics, Lanzhou University, Lanzhou 730000, China (e-mail: houmch20@lzu.edu.cn; zhlliu19@lzu.edu.cn).

Hengji Li is with the Lanzhou Information Center Northwest Institute of Eco-Environment and Resources, Chinese Academy of Sciences, Lanzhou 730000, China (e-mail: lihengji@llas.ac.cn).

Chenyu Lu is with the College of Geography and Environment Sciences, Northwest Normal University, Lanzhou 730000, China (e-mail: luchenyu@nwnu.edu.cn).

Digital Object Identifier 10.1109/JSTARS.2021.3105897

I. Introduction

As ONE of the most important components of the earth's terrestrial ecosystem, vegetation has the function of connecting ecological elements, such as the atmosphere, soil, and water, thereby playing an extremely important role in regional climate regulation, human settlements maintenance, carbon sequestration, oxygen release, biodiversity protection, and other ecological service functions, and it can provide a strong guarantee for the natural ecosystem and human life [1]–[5]. At present, the monitoring and attribution analysis of large-scale and long-term vegetation changes has become an important part of the research on global changes and ecological environmental protection [6]. Such research can provide a scientific basis for humans to undertake reasonable land use and human settlements construction [7], [8].

The normalized difference vegetation index (NDVI) is an effective indicator of large-scale vegetation cover changes [9]–[14], can represent the surface vegetation cover and vegetation growth, and can be used to monitor vegetation changes and explain the impact of weather/climate events on the human settlements [15]–[17]. Currently, the most used NDVI data include the SPOTVGT NDVI [18], advanced very high-resolution radiometer (AVHRR) NDVI [19], and Moderate Resolution Imaging Spectroradiometer (MODIS) NDVI [20]. The use of different NDVI products may cause certain differences in the results, but they still have obvious advantages in the studies on large-scale vegetation cover changes and their causes as well as in land cover identification [21]. Globally, vegetation activities have exhibited an increasing trend [22], and the vegetation cover of the Eurasian continent [23], China [24], and the eastern region of China [25] has shown certain changes. Vegetation dynamics are affected by natural factors and human activities, and climate is the main factor that determines the distribution of vegetation types. The most significant climatic factors are temperature, precipitation, and sunshine duration [26].

In recent years, the use of a variety of RS data to study the response relationship between vegetation NDVI and climate factors has become a hot topic. For example, Paruelo and Lauenroth [27] studied the grasslands and shrubs in North America and found that temperature and precipitation were the two most important climatic factors controlling the regional variation in the changes in the vegetation cover range during the year. Milich and Weiss [28] found that the amount of precipitation played a decisive role in seasonal NDVI, and when the precipitation reached a certain level, the correlation between the two was significant. Ichii *et al.* [29] studied the mid-high latitudes of the Northern Hemisphere and found that the interannual variations in NDVI in spring and summer were significantly correlated with the temperature, whereas in the semiarid area, the vegetation variations had a good correlation with the temperature and precipitation. Lamchin *et al.* [30] analyzed the correlations between the seasonal variations in vegetation NDVI and temperature, precipitation, evapotranspiration, and other factors in Asia during 1982–2014 and found that temperature changes were the most important factor causing vegetation NDVI changes in Asia. Richard and Poccard [31] used the NOAA/AVHRR time-series data to study the response of vegetation to seasonal and annual precipitation fluctuations in southern Africa. Suzuki *et al.* [32] used the monthly mean NDVI between 1987 and 1991 to study the seasonal variation patterns of NDVI as temperature and precipitation changed in Siberia and its surrounding areas. Based on the continuous 69-month NOAA time-series data from 1985 to 1990 and the monthly mean temperature and precipitation data during the same period, Sun *et al.* [33] analyzed the correlations between vegetation cover changes and climate factors, and the results confirmed the pattern of vegetation cover change over time and the quantitative relationships between vegetation cover change and temperature and precipitation in China. Liu *et al.* [34] analyzed the trends and interaction relationships between NDVI and climatic factors for the entire China Loess Plateau and separate areas with different plant cover types in 2000–2015. They found that there were no significant correlations between NDVI and climatic factors, such as temperature, sunshine, precipitation, and relative humidity in the entire China Loess Plateau. However, in areas with different vegetation cover types, climatic factors had significant effects on NDVI, and there were obvious differences between areas with different vegetation cover types. Droughts triggered by rising temperatures in the Northern Hemisphere played a significant role in the decline in vegetation cover in some high-latitude places in the 1980s [35]. Over the past 30 years, global warming has promoted vegetation restoration in the central and southeastern regions of China Loess Plateau but has inhibited vegetation restoration in the northwest regions of China Loess Plateau [36].

The Yellow River Basin is an important ecological barrier and economic zone in China, is also an important region for precision poverty alleviation, and plays a key role in China's economic and social development and ecological security [37]. In 2019, efforts to protect the ecological environment of the Yellow River Basin and undertake high-quality development were proposed. These became a major national strategy along with the coordinated development of the Beijing–Tianjin–Hebei region, the development of the Yangtze River Economic Belt, construction in the Guangdong–Hong Kong–Macau Greater Bay Area, and the integrated development of the Yangtze River Delta.

In recent years, on the background of global climate change and rapid regional socioeconomic development, the vegetation cover of the Yellow River Basin has undergone profound changes [38], [39]. Other prominent issues in the basin are the grim situation of water resource security and the fragile human ecological environment [40], [41]. Investigating the characteristics of vegetation and climate changes in the Yellow River Basin and the response relationship between the two is highly important to ecosystem regulation, improvement of the human ecological environment, and disaster prevention and mitigation.

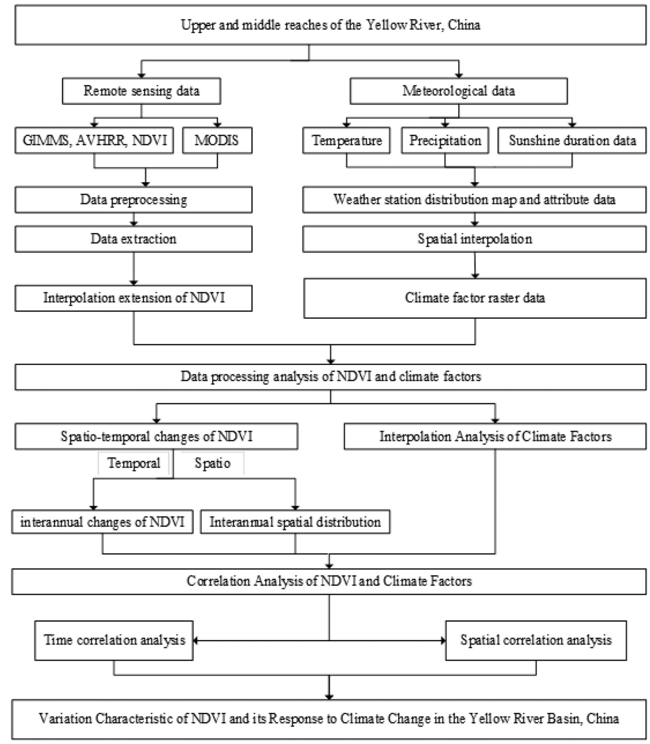

Fig. 1. Technology roadmap.

Based on RS and GIS data, this study analyzed the variation pattern of vegetation NDVI in the middle and upper reaches of the Yellow River in 1989–2018 and analyzed the response relationships between vegetation NDVI and climate factors based on meteorological data, such as temperature, precipitation, and sunshine duration. This study aimed to provide a theoretical basis for the ecological protection and high-quality development of the Yellow River basin, especially around the upper and middle reaches of the Yellow River. Technology roadmap is shown in Fig. 1.

II. Materials and Methods

A. Studied Cases

The Yellow River originates in the Qinghai–Tibet Plateau, flows through nine provinces, such as Qinghai, Sichuan, and Gansu, and has a total length of 5464 km and a watershed area of 795 000 km^2. The Yellow River Basin is an important irrigated agricultural area and an important industrial belt in China, holding 12.5% of China's population. However, the natural conditions in most areas are complicated, which makes them ecologically fragile and unstable [42]. The middle and upper reaches of the Yellow River start from the headwaters of the Yellow River in the west and extend to the western border of

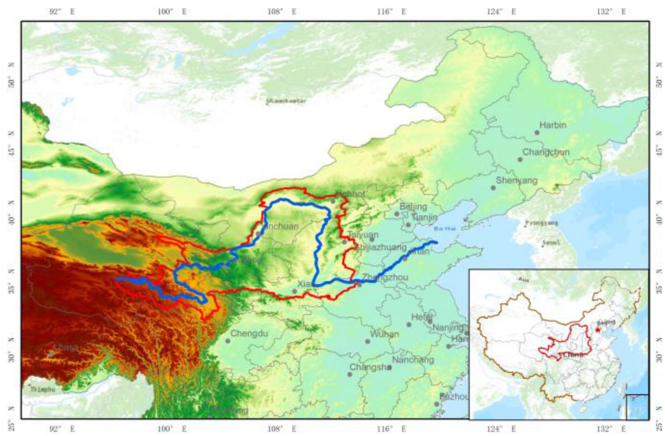

Fig. 2. Magnetization location of the studied areas.

the North China Plain in the east, the northern foot of the Qinling Mountains to the south, and the Yin Mountain to the north. They are between 95°53′–113°35′E and 32°12′–41°50′N, with a total area of 723 100 km^2, accounting for 92% of the Yellow River basin. The ecological environment quality of the middle and upper reaches of the Yellow River directly determines the environmental status of the downstream regions, so the middle and upper reaches of the Yellow River have a very important strategic significance in geographical location and ecological protection. The middle and upper reaches of the Yellow River pass through the China Loess Plateau, where the terrain is high in the northwest and low in the southeast (see Fig. 2), with typical characteristics of the continental monsoon climate, i.e., it is hot and rainy in summer and cold and dry in winter. This area is mostly covered with loose loess soil and is affected by concentrated precipitation, deforestation and land reclamation, urban construction, and other factors, making it a typical region of China with a fragile ecological environment [43].

B. NDVI Data

The RS NDVI data include the Global Inventory Modeling and Mapping Studies (GIMMS) and MODIS datasets. The GIMMS AVHRR NDVI dataset is from the Environmental and Ecological Science Data Center for National Natural Science Foundation of West China.[1] The data are from sensors of NOAA-11, NOAA-9 (deorbiting), and NOAA-14. The image projection format is ALBERS equal-area projection. The time resolution is 15 d. The spatial resolution is 8 km. The period for time-series data is 1981–2003. A total of 22 periods, the first and second halves of each July from 1989 to July 1999, were selected for study, and monthly maximum NDVI was calculated by maximum-value composite (MVC). Then, vector boundaries of the middle and upper reaches of the Yellow River were used to extract the study area in ArcMap. The MODIS dataset is from the Global Monitoring and Modeling Group of the National Aeronautics and Space Administration (NASA). The MOD13A3 vegetation index product set with a spatial resolution of 1 km, a temporal resolution of 1 month, and a time scale of January 2000 to December 2018 was used. MOD13A3 data of four scenarios, including h25v05, h26v04, h26v05, and h27v05, were selected. The MODIS Reprojection Tool software of NASA was used for the batch processing of MODIS data, including image mosaic, projection, and coordinate system transformation. Data were uniformly converted to ALBERS equal-area projections and the World Geodetic System 1984 coordinate system, the HDF format was converted to TIFF format, and then the vector boundary of the study area was captured by ArcMap. The GIMMS and MODIS datasets were smoothed and denoised by Savitzky–Golay (S-G) filtering. The spatial resolution of the GIMMS dataset is 8 km, and that of the MODIS dataset is 1 km. Since the resolutions of the two are different, the resolution of the MODIS data was resampled to 8 km using the resampling tool in ArcGIS so that the two were consistent in space. Then, TIMESAT3.1 software supported by MATLAB was used to randomly select the vegetation pixels in the middle and upper reaches of the Yellow River, and S-G filtering was used to reconstruct the vegetation NDVI time-series data. After S-G filtering, the vegetation NDVI time-series data were relatively smooth, so they sufficiently preserved the useful information for the time-series curve study and eliminated the adverse factors in the data.

The meteorological data were from the China Meteorological Data Service Center. Meteorological data of the middle and upper reaches of the Yellow River and the surrounding areas from 1989 to 2018, including temperature, precipitation, sunshine duration, and other meteorological data, were selected from the annual climatological dataset of China Ground International Exchange Station. After removing some outliers, the mean value method was used to calculate the mean temperature, mean precipitation, and sunshine duration for the selected meteorological stations from 1989 to 2018 (30 years). The *XY* data were added into ArcGIS and exported as .shp files. The ordinary kriging interpolation was used to interpolate the mean precipitation and sunshine duration. Since temperature is greatly affected by altitude, the cokriging interpolation in the statistical analysis tools in ArcGIS was used to interpolate the mean temperature. The altitude of each meteorological station was taken as the covariate, and the interpolation analysis charts of three climate factors were obtained to analyze spatiotemporal variations.

C. Methodology

MVC was done to maximize the 10-day data to reduce the impact of clouds, atmosphere, and solar elevation angle on the image data. In this study, MVC was applied to the 15-day GIMMS NDVI to obtain the monthly NDVI data

$$\mathrm{NDVI}_{\mathrm{month}} = \max(\mathrm{NDVI}_i, \mathrm{NDVI}_j) \quad (1)$$

where $\mathrm{NDVI}_{\mathrm{month}}$ is the monthly NDVI, NDVI_i is the NDVI for the first half of one month, and NDVI_j is the NDVI for the second half of one month.

The mean value method was used to calculate the mean temperature, mean precipitation, and sunshine duration at each meteorological station from 1989 to 2018, which were used

[1] [Online]. Available: http://westdc.westgis.ac.cn

TABLE I
CRITICAL VALUES FOR THE SIGNIFICANCE TEST OF CHANGE TRENDS

f \ a	0.1	0.05	0.01
28	2.894	4.196	7.636

TABLE II
CRITICAL VALUES FOR THE SIGNIFICANCE TEST OF CORRELATION COEFFICIENTS

f \ a	0.1	0.05	0.01
28	0.30606	0.36101	0.46289

TABLE III
VEGETATION COVER LEVELS

Mean NDVI	Level
<0.1	Low-vegetation-cover area (Low area)
0.1-0.3	Medium/low-vegetation-cover area (Medium/low area)
0.3-0.5	Medium-vegetation-cover area (Medium area)
0.5-0.7	Medium/high-vegetation-cover area (Medium/high area)
>0.7	High-vegetation-cover area (High area)

for interpolation analysis of climatic factors to facilitate the subsequent analysis of the relationships between vegetation NDVI changes and climate factors.

Unitary linear regression analysis was done to simulate the trend of NDVI variation on the pixel scale from 1989 to 2018, and the trend of vegetation variation for each pixel for 30 years was regressed. The calculation formula is

$$\text{Slope} = \frac{n\sum_{i=1}^{n} iY_i - \sum_{i=1}^{n} i \sum_{i=1}^{n} Y_i}{n\sum_{i=1}^{n} i^2 - \left(\sum_{i=1}^{n} i\right)^2} \tag{2}$$

where n is the year serial number, i is the year number, Y_i is the NDVI of the ith year, and Slope is the trend of NDVI in a certain pixel during the study period. Slope > 0 indicates that the vegetation in the pixel has a positive upward trend, and Slope < 0 indicates that the vegetation in the pixel has a downward trend. At the same time, the F-test was used to check the significance level of the vegetation trend

$$F = U \times \frac{n-2}{Q} \tag{3}$$

where $U = \sum_{i=1}^{n} (\hat{y}_i - \bar{y})^2$ is the regression sum of squares, $Q = \sum_{i=1}^{n} (y - \hat{y}_i)^2$ is the residual sum of squares, y_i is the value of a certain factor in the ith year, $\hat{y}_i$ is the regression value of this factor, and $\bar{y}$ is the n-year mean of this factor. The distribution table of the F-test is shown in Table I. In the table, f represents the degrees of freedom. Its value is $n - 2$, where n is the number of samples. In this study, n is 30, so f is 28. The superscript a represents different confidence levels, and the number in the table represents the critical value of the correlation coefficient ($p = 0$) at different confidence levels, namely, F_a. A value of $F_a <$ 4.196 indicates basically stable, $4.196 < F_a < 7.636$ indicates mild change, and $F_a > 7.636$ indicates significant change.

Pearson correlation analysis was used to calculate the correlation coefficients between annual mean NDVI and annual mean temperature, precipitation, and sunshine duration to reflect the dynamic changes in vegetation NDVI of the study area and the response degree of climate factors. The calculation formula is

$$r_{xy} = \frac{\sum_{i=1}^{n} (x_i - \bar{x})\ (y_i - \bar{y})}{\sqrt{\sum_{i=1}^{n} (x_i - \bar{x})^2 \sum_{i=1}^{n} (y_i - \bar{y})^2}} \tag{4}$$

where x_i and y_i are the mean NDVI of year i and the meteorological data of the same period, $\bar{x}$, $\bar{y}$ are the multiyear mean of NDVI and the mean of meteorological data during the study period, and r_{xy} is the correlation coefficient between NDVI and a climatic factor. In this study, the T-test was used to test the significance of the correlation coefficient.

The values of f and a are the same in Tables I and II, and the number represents the critical value of the correlation coefficient ($p = 0$) at different confidence levels, namely, r_a. An absolute value $|r_a| < 0.36101$ indicates no significant correlation; $0.36101 < |r_a| < 0.46289$ shows a significant correlation; and $|r_a| > 0.46289$ indicates a highly significant correlation.

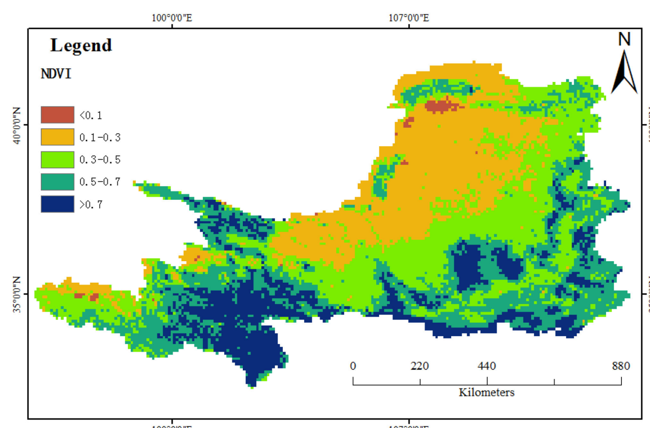

Fig. 3. Levels of the annual mean vegetation cover in the middle and upper reaches of the Yellow River between 1989 and 2018.

III. RESULTS

A. Spatial Distribution Characteristics of Vegetation NDVI

In ArcGIS, statistical tools for pixels were used to obtain the mean NDVI over the 30 years in the middle and upper reaches of the Yellow River. Negative NDVI indicates that the ground cover was clouds, water, snow, or others; 0 indicates rocks or bare soil; and positive value indicates vegetation cover. The higher the NDVI, the higher the vegetation cover. This study divides the vegetation cover into five levels (see Table III).

The vegetation NDVI levels of the middle and upper reaches of the Yellow River from 1989 to 2018 were obtained (see Fig. 3). The low-vegetation-cover area (low area) accounted for

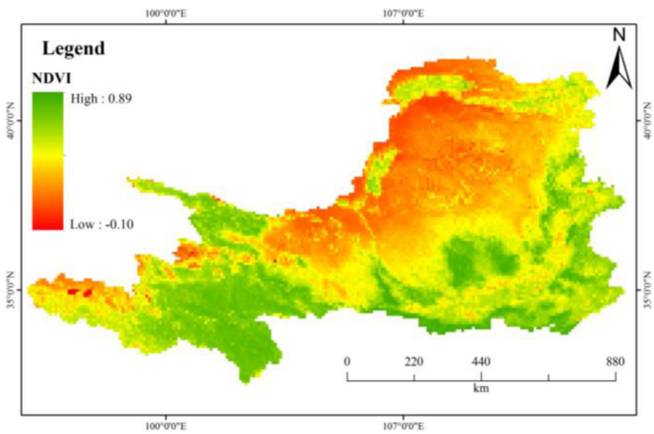

Fig. 4. Annual mean NDVI distribution in the middle and upper reaches of the Yellow River between 1989 and 2018.

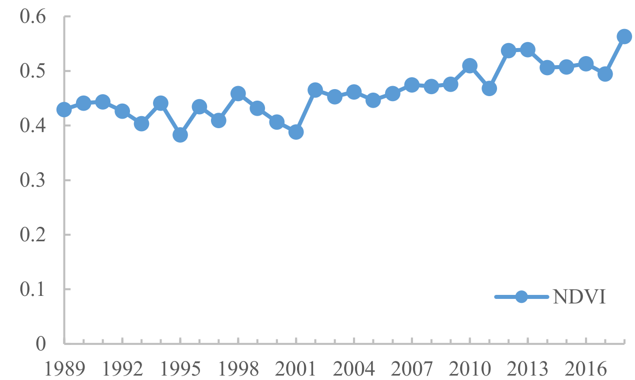

Fig. 5. Trend of interannual variation in annual mean NDVI in the middle and upper reaches of the Yellow River between 1989 and 2018.

approximately 0.66% of the entire study area, the medium/low-vegetation-cover area (medium/low area) accounted for approximately 25.75%, the medium-vegetation-cover area (medium area) accounted for approximately 31.28%, the medium/high-vegetation-cover area (medium/high area) accounted for approximately 26.43%, and the high-vegetation-cover area (high area) accounted for approximately 15.89%. It can be seen that the medium and medium/high areas were the largest. The annual mean NDVI is shown in Fig. 4. The 30-year mean NDVI in the upper and middle reaches of the Yellow River was 0.46, so the overall vegetation cover level was moderate, showing an upward trend from northeast to southwest. The lowest percentage of vegetation cover was found in the Shizui Mountain area in the northeast, followed by the Qingshui River, Kushui River, endorheic basins, and others. The highest percentages of vegetation cover were found in Baoji, Xianyang, Xi'an, Shangluo, Tongguan, Sanmenxia, and Luoyang, which are located at the tributaries of Wei River, followed by Maqu, the Tao River, and the Yiluo River in the southwest. In general, the vegetation cover in the upper and middle reaches of the Yellow River was moderate.

As for tributaries, the annual mean NDVI of the areas of Daxia River and Tao River was the highest, reaching 0.67, and most parts belonged to medium/high or high areas. The mean NDVI of the Yiluo River was relatively high, approximately 0.65, and most parts belonged to medium/high areas. The mean NDVI of areas from Shizui Mountain to the south bank of Hekou town was the lowest, approximately 0.21, and most parts belonged to medium/low or low areas, indicating low vegetation cover and a poor ecological environment. Therefore, the green areas should be appropriately increased. The mean NDVI of the endorheic basins was approximately 0.21, a relatively low vegetation cover, putting these basins in the medium/low category, and the vegetation condition was very poor. In addition, the mean NDVI in the areas of Qingshui River, Kushui River, and Lanzhou to Shizui Mountain was also relatively low, putting most of their area in the medium/low category, and the vegetation condition was moderate.

TABLE IV
VEGETATION CHANGE LEVELS

Slope/p	Level
Slope<0, p<0.01	Significantly reduced
Slope<0,0.01<p<0.05	Slightly reduced
p>0.05	basically stable
Slope>0,0.01<p<0.05	Slightly increased
Slope>0, p<0.01	Significantly increased

B. Temporal Variation Characteristics of Vegetation NDVI

The annual mean NDVI data of the middle and upper reaches of the Yellow River from 1989 to 2018 derived from ArcGIS were used to represent the vegetation cover, and the trend of annual mean NDVI was analyzed (see Fig. 5). The raster calculator in ArcGIS was used to calculate the slope of NDVI, and then the trend of vegetation NDVI in each pixel for 30 years was regressed to simulate the interannual trend of NDVI at the pixel scale. The significance of the overall linear relationship of the regression equation of Slope was tested by the F-test. Based on the test results, we divided the trend of the vegetation change into five levels (see Table IV) and drew the multiyear vegetation trend plot for the study area (see Fig. 6).

As shown in Figs. 5 and 6, in 1989–2018, the annual mean NDVI of the middle and upper reaches of the Yellow River showed an overall increasing trend, and the vegetation cover showed a significant trend of improvement. The mean NDVI was 0.46, the highest annual mean NDVI was 0.56 (in 2018), and the lowest was 0.38 (in 1995). The vegetation covers gradually increased with fluctuations in 1989–1998 and then declined until 2001, when the annual mean NDVI was near the minimum of 0.38. In 2001–2002, the annual mean NDVI increased rapidly, the growth rate reaching 19.67%. After 2002, the vegetation covers significantly increased with fluctuations and reached its peak in 2018. In the past 30 years, the growth rate of vegetation cover in the study area reached 31.28%, indicating that the local governments and society paid attention to the protection

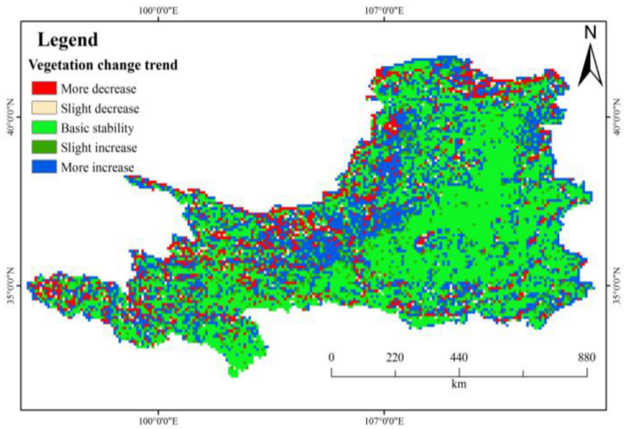

Fig. 6. Trend of vegetation in the middle and upper reaches of the Yellow River between 1989 and 2018.

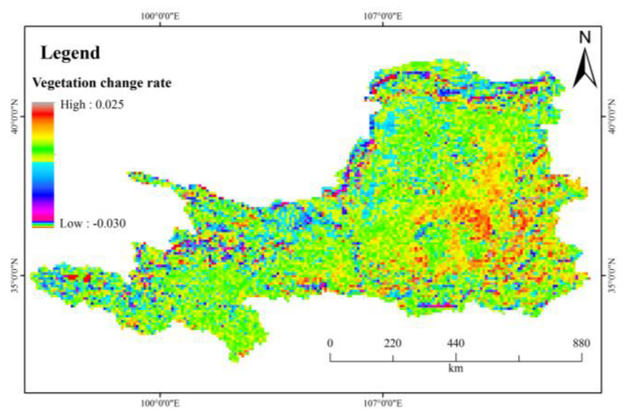

Fig. 7. Slope of NDVI variation in the middle and upper reaches of the Yellow River between 1989 and 2018.

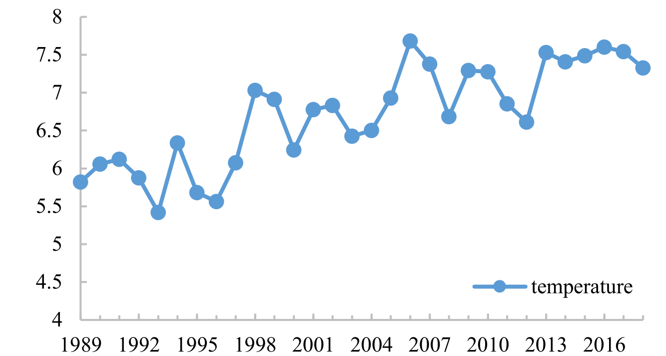

Fig. 8. Trend of interannual variation in annual mean temperature in the middle and upper reaches of the Yellow River between 1989 and 2018.

and control of the ecological environment and achieved certain success in building an ecological civilization.

According to the slope of NDVI over the past 30 years (see Fig. 7), the overall vegetation cover in the middle and upper reaches of the Yellow River increased. A total of 2243 pixels had Slope < 0, accounting for 18.17% of the total number of pixels, and were mainly distributed in the trunk stream area of Heyuan–Longyangxia to Lanzhou and the area of Xia River–north bank of Hekou Town. A total of 10 099 pixels had Slope > 0, accounting for 81.83% of the pixels, and were mainly distributed in the middle reach of the Yellow River.

As for the trend of vegetation cover over the past 30 years, the vegetation in the area of Lanzhou to the Xia River–Qingshui River–Kushui River showed a significant increasing trend, including 3619 pixels (accounting for 29.29% of the pixels) and with the highest vegetation change rate of 0.025. The areas with a slight increase in vegetation cover were scattered. There were 1079 such pixels, accounting for 8.74% of the pixels. There were 6007 pixels with a basically stable vegetation cover, accounting for 48.67% of the pixels. The areas with a slight decrease in vegetation cover were mainly distributed in the areas of Heyuan–Baoji Gorge of the Wei River to Tongguan–Xiheyan–Shizui Mountain to the north bank of Hekou town, totaling 271 pixels, or 2.2% of the total number of pixels. The areas with significantly reduced vegetation cover were mainly distributed in the upper reach of the Yellow River. There were 1370 such pixels, accounting for 11.1% of the pixels, with the lowest change rate reaching –0.0295. There were 12 342 pixels in the entire study area, and the mean vegetation change rate was approximately 0.004.

For each tributary area, the vegetation cover in the area of Sanmenxia to Xiaolangdi showed an overall increasing trend, with a total of 94 pixels, and the mean vegetation growth rate was the highest, reaching 0.0084. The vegetation cover in the truck stream areas of the right bank downstream of the Fen River and Wubao–Xiaolangdi to Huayuankou showed an increasing trend, with a mean growth rate > 0.007. The vegetation cover in the truck stream area of the right bank upstream of the Yingdan River, Wubao–Upstream of the Beiluo River–Longmen to Sanmenxia, and the left bank upstream of Zhangjia Mountain of the Wei River–Hekou town to Longmen showed an increasing trend. There were 912 pixels in the area of the north bank of Shizui Mountain to Hekou Town, where the overall vegetation cover was basically stable, with the lowest mean vegetation growth rate of approximately 0.0013. The vegetation cover was also relatively stable in the truck stream area of Lanzhou to Xiaheyan and Longyangxia–Lanzhou. There was no significant increase or decrease, and the mean growth rate of vegetation was < 0.002. The mean vegetation change rate of all areas in the middle and upper reaches of the Yellow River was positive, that is, the vegetation cover of each area has improved over the past 30 years, with slight or obvious growth.

C. Correlations Between Vegetation NDVI and Climatic Factors

By analyzing the kriging interpolation plots of mean temperature, mean precipitation, and sunshine duration at each meteorological station in the middle and upper reaches of the Yellow River over 30 years, the spatiotemporal variation characteristics of these three climatic factors were obtained.

According to the spatial distribution (see Fig. 8) and the trend of the interannual variation (see Fig. 9) of mean temperature,

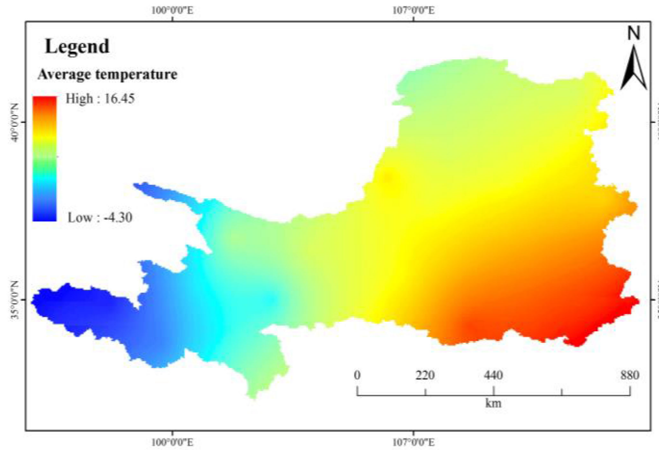

Fig. 9. Spatial distribution of annual mean temperature in the middle and upper reaches of the Yellow River between 1989 and 2018.

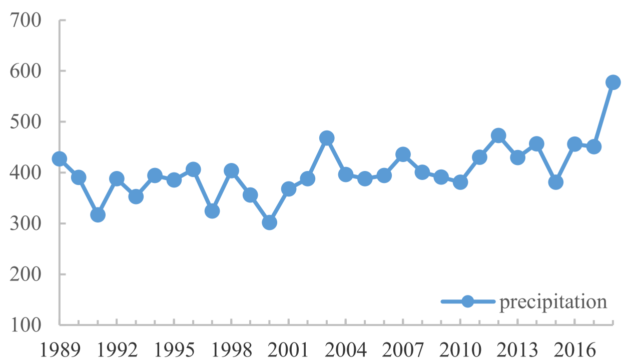

Fig. 10. Trend of interannual variation in average annual precipitation in the middle and upper reaches of the Yellow River between 1989 and 2018.

there was a clear upward trend in temperature over the past 30 years, with a mean annual temperature of 6.71 °C. The highest annual mean temperature was 7.69 °C in 2006 and was 1.28 °C higher (approximately 19.1%) than the mean annual temperature, and the lowest annual mean temperature was 5.42 °C in 1993 and was 1.29 °C lower (approximately 19.2%) than the mean annual temperature. The lowest mean temperature was approximately –4.3 °C and was mainly found in the southern areas of Qinghai, where the highest mean temperature was approximately 16.45 °C and was mainly found in the southwestern part of Shanxi Province and the Wei River area. In terms of space, the temperature distribution in the past 30 years was generally low in the southwest and high in the southeast. In particular, the areas with low mean temperature were mostly distributed in the high-altitude Madio and Darlag regions, whereas the areas with high mean temperature were mostly distributed in low-altitude regions such as Yuncheng and the Jing River.

According to the spatial distribution (see Fig. 10) and the trend of interannual variation (see Fig. 11) of mean precipitation, the overall precipitation exhibited a gradual upward trend over the past 30 years, with a mean annual precipitation of 403.81 mm. The highest annual mean precipitation was 577.9 mm (in 2018), which was 174.09 mm higher (approximately 43.1%) than the mean annual precipitation. The lowest annual mean precipitation was 301.82 mm in 2000 and was 101.99 mm lower (approximately 25.3%) than the mean annual precipitation. Except for the relatively large increments in 2000–2003 and 2017–2018, the changes in other years were relatively small, so the overall precipitation was relatively stable.

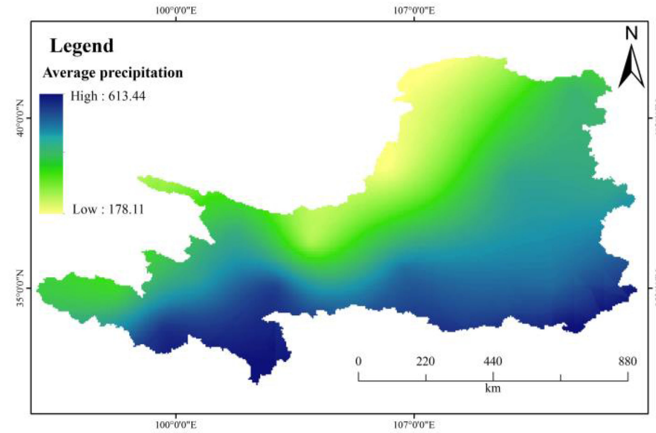

Fig. 11. Spatial distribution of interannual variation in annual mean precipitation in the middle and upper reaches of the Yellow River between 1989 and 2018.

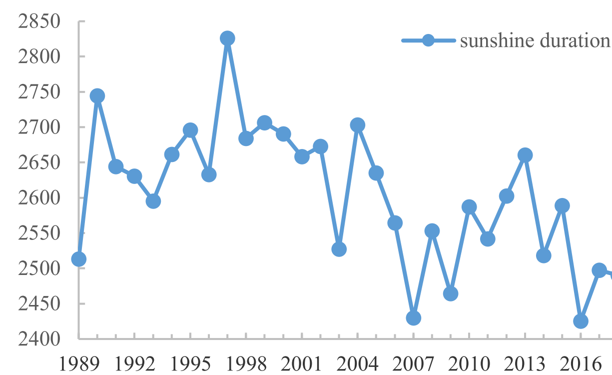

Fig. 12. Trend of interannual variation in annual mean sunshine duration in the middle and upper reaches of the Yellow River between 1989 and 2018.

There was an overall pattern of gradually decreasing precipitation from southeast to northwest. The precipitation in the southern part was generally high (> 600 mm), whereas the precipitation in the northern part was low. The lowest precipitation was 178.114 mm, which was mainly found in the Inner Mongolia Autonomous Region, and the highest precipitation was 613.436 mm, which was mainly found in the area south to the Maqu and Yiluo River area.

According to the spatial distribution (see Fig. 12) and the trend of interannual variation (see Fig. 13) of mean sunshine duration, the mean sunshine duration in the past 30 years had a significant decreasing trend, with a mean annual sunshine duration of 2604.97 h. The highest annual mean sunshine duration was 2825.95 h (in 1997), 220.98 h (approximately 8.5%) more than the mean annual sunshine duration. The lowest annual mean

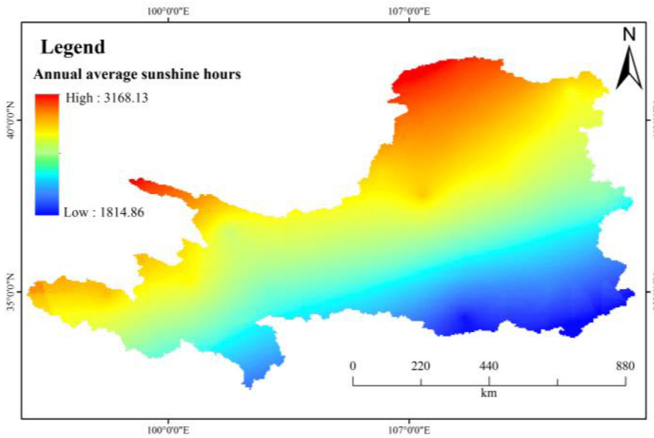

Fig. 13. Spatial distribution of interannual variation in annual average sunshine hours in the middle and upper reaches of the Yellow River between 1989 and 2018.

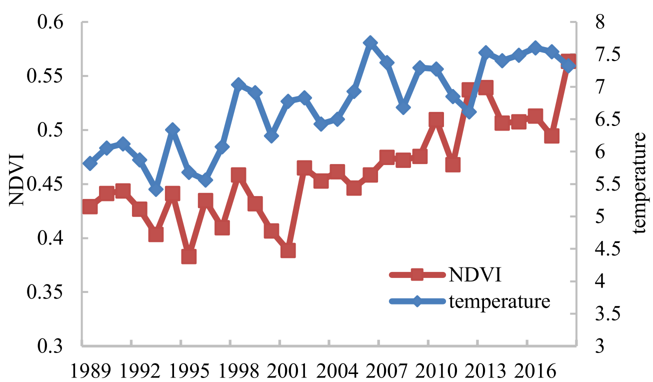

Fig. 14. Interannual variational curves of NDVI and temperature in the middle and upper reaches of the Yellow River between 1989 and 2018.

sunshine duration was 2242.61 h in 2016, 179.36 h (approximately 6.9%) less than the mean annual sunshine duration. Over 1989–1999, the annual mean sunshine duration increased significantly (approximately 231.12 h), and in 2004–2007, it decreased significantly (approximately 273.4 h).

There was an overall pattern of gradually increasing sunshine from southeast to northwest. The minimum sunshine duration was 1814.86 h, which mainly occurred in the area of Baoji Gorge of Wei River to Tongguan and the Yiluo River area, and the maximum sunshine duration was 3168.13 h, which mainly occurred in the area north of the Xiangtang in the Datong River and the Shizui Mountain to the north bank of Hekou Town.

1) Temporal Correlations Between Vegetation NDVI and Climatic Factors: Fig. 14 shows that the annual mean NDVI was highly correlated with temperature over the past 30 years. In 1989–1995, the correlation coefficient between the annual mean NDVI and temperature reached 0.794, and the trends of the two tended to be consistent. In 1995–2002, the trends of the two were mostly opposite, with a correlation coefficient of only 0.287. In 2002–2004, the two had relatively similar trends, and in 2005–2013, the correlation between the two was relatively small, with a correlation coefficient of –0.022. In 2013–2017, the two had relatively similar trends, and the periods of increase and decrease were the same. In 2017–2018, the NDVI showed an obvious increasing trend, whereas the temperature showed a weak decreasing trend. Overall, over the past 30 years, the annual mean NDVI of the middle and upper reaches of the Yellow River showed a positive correlation with the annual mean temperature, with a correlation coefficient of 0.710.

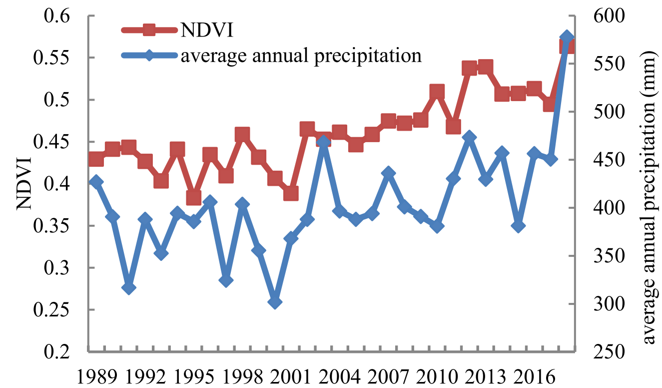

Fig. 15. Interannual variational curves of NDVI and average annual mean precipitation in the middle and upper reaches of the Yellow River between 1989 and 2018.

Fig. 15 shows that the trends of the annual mean NDVI and precipitation had temporal differences over the past 30 years. In 1989–1992, the trends of the two were completely opposite. In 1992–2000, the trends of the two were relatively consistent, with the same periods of increase and decrease and a correlation coefficient of 0.507. In 2000–2001, the annual mean NDVI showed a decreasing trend, whereas the annual mean precipitation showed a significant increasing trend. In 2001–2002, the two had similar trends. In 2002–2004, the trends of the two were opposite, but the variation in the annual mean NDVI was relatively small. In 2004–2008, the trends of the two were similar, with the same periods of increase and decrease. In 2008–2011, the trends of the two were opposite. In 2011–2012, both showed an upward trend. In 2012–2015, the trends of the two were opposite, with a correlation coefficient of 0.427. In 2015–2018, the trends of the two were similar, and the annual mean NDVI had relatively small variations. Overall, over the past 30 years, in the middle and upper reaches of the Yellow River, the annual mean NDVI showed a positive correlation with the annual mean precipitation, with a correlation coefficient of 0.708.

Fig. 16 shows that the trends of the annual mean NDVI and sunshine duration had temporal differences over the past 30 years. In 1990–1991, the trends of the two were opposite, and in 1989–1994, the trends of the two were essentially the same. In 1994–1999, they were opposite again. In 1999–2005, they returned to trending similarly, with the same periods of increase and decrease, but the variations were greatly different. In 2001–2002, the annual mean NDVI increased by 19.67%, whereas the sunshine duration increased by only 0.55%. In 2005–2002, the trends of the two were opposite, and in 2009–2015, they were similar, with same periods of increase or decrease and a correlation coefficient as high as 0.8. In 2016–2018, the trends

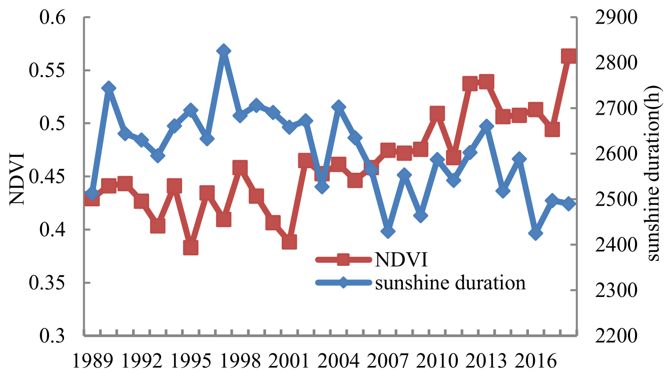

Fig. 16. Interannual variational curves of NDVI and sunshine duration in the middle and upper reaches of the Yellow River between 1989 and 2018.

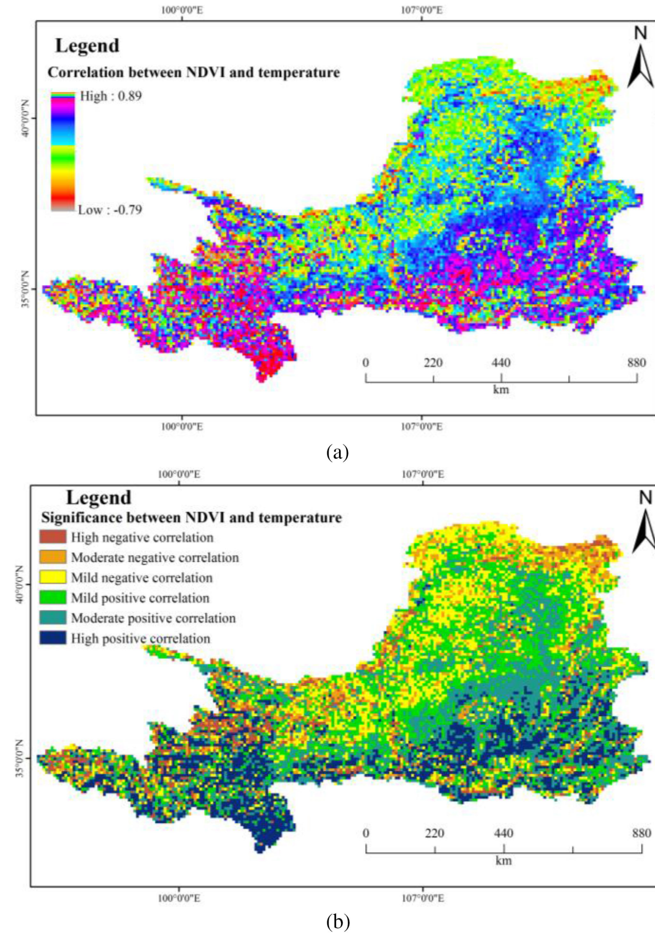

Fig. 17. Significance between NDVI and temperature in the middle and upper reaches of the Yellow River between 1989 and 2018.

of the two were opposite, with a weak negative correlation and a correlation coefficient of –0.156. Overall, over the past 30 years, in the middle and upper reaches of the Yellow River, the annual mean NDVI showed a negative correlation with sunshine duration, with a correlation coefficient of –0.510.

2) Spatial Correlations Between Vegetation NDVI and Climatic Factors: Based on the annual mean NDVI, temperature, precipitation, and sunshine duration from 1989 to 2018, combined with the Pearson correlation analysis, the spatial distributions of the correlation coefficients of NDVI and temperature, precipitation, and sunshine duration were obtained using the raster calculator in ArcGIS (see Figs. 17(a), 18(a), and 19(a), respectively), and the spatial distributions of the significance of the correlation coefficients of NDVI and temperature, precipitation, and sunshine duration were obtained by the *t*-test (see Figs. 17(b), 18(b), and 19(b), respectively).

Fig. 17 shows that in the past 30 years, the correlation coefficient between vegetation NDVI and temperature exhibited a gradual increasing trend from northeast to southwest, 81.15% of the total area had a positive correlation coefficient, and 18.85% of the total area had a negative correlation coefficient. The latter were mainly distributed in the areas of the north bank of Hekou town and part of the Lanzhou to Xiahe River area in northeast China. The areas with an extremely positive or positive correlation between vegetation NDVI and temperature accounted for approximately 41.34% of the study area and were mainly distributed in the southwest areas of Darlag, Maqu, Yanglongxia, Hezuo, Yan'an, Yuncheng, and the Wei River. The areas with an extremely negative or negative correlation between vegetation NDVI and temperature accounted for approximately 3.93% of the study area and were mainly distributed in the truck stream area from Yanglongxia to Lanzhou. In general, in the southwest and south regions of the upper and middle reaches of the Yellow River, the vegetation NDVI had a strong positive correlation with temperature, whereas the correlations in other regions were weak. In terms of each tributary area, the vegetation NDVI in the area from Sanmenxia to the Xiaolangdi had the strongest correlation with temperature, which indicates the NDVI was more significantly affected by temperature here than other areas. In addition, the correlation coefficients between NDVI and temperature in the truck stream area in the upstream of the Beiluo River and Xiaolangdi to Huayuankou and Qindan River area all were over 0.4. In the area from Shizui Mountain to the north bank of Hekou town, the correlation between NDVI and temperature was the weakest, indicating that compared to other areas, the vegetation NDVI in this area was less affected by temperature. In addition, the vegetation NDVI in the areas of Lanzhou–Xiaheyan and Xiaheyan–Shizui Mountain was relatively less affected by temperature.

Fig. 18 shows that, in the past 30 years, the correlation coefficient between vegetation NDVI and precipitation exhibited a gradual increasing trend from southwest to northeast. The areas with positive correlation coefficients accounted for 79.11% of the study area and were mainly distributed in the middle reach of the Yellow River, and the areas with negative correlations accounted for 28.89% of the study area and were mainly distributed in the southwest part and the Wei River area. The areas with an extremely positive or positive correlation between vegetation NDVI and precipitation accounted for approximately 19.63% of the study area and were mainly distributed in the areas of Urad Middle Banner, Hohhot, Wubao, Yulin, Kongtong, and Gaolan. The areas with an extremely negative or negative correlation between vegetation NDVI and temperature accounted

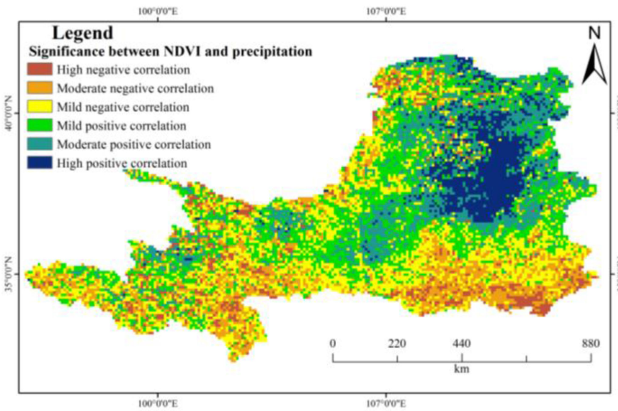

(a)

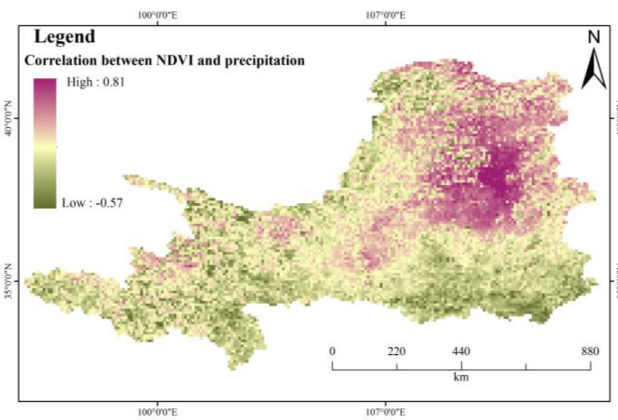

(b)

Fig. 18. Significance between NDVI and precipitation in the middle and upper reaches of the Yellow River between 1989 and 2018.

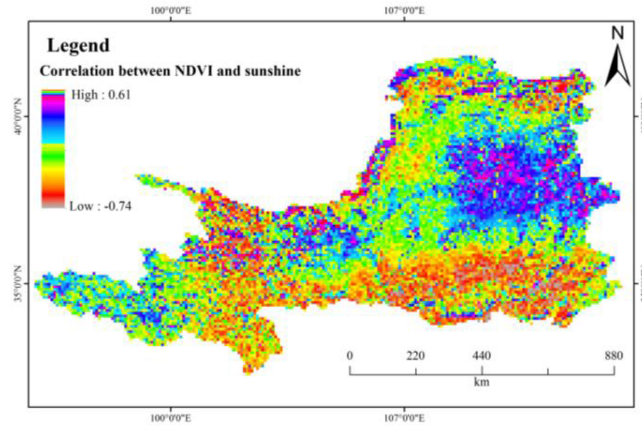

(a)

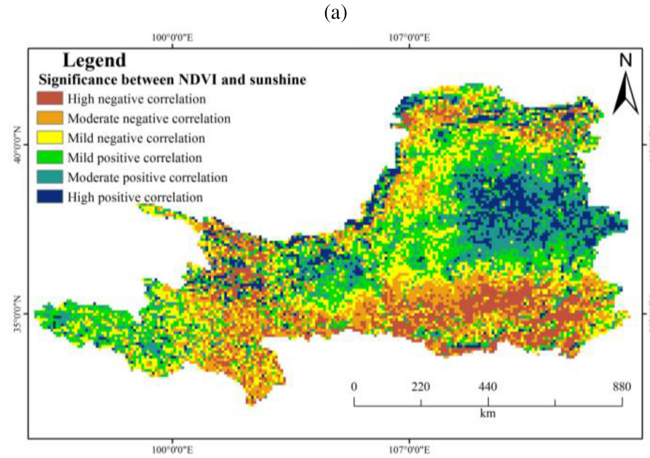

(b)

Fig. 19. Significance between NDVI and sunshine duration in the middle and upper reaches of the Yellow River between 1989 and 2018.

for approximately 0.42% of the study area and were mainly distributed in the area around the Wei River. Overall, in the upper and middle reaches of the Yellow River, except for the northeastern part showing a strong positive correlation between NDVI and precipitation, the correlation was relatively weak. Focusing on each tributary area, the vegetation NDVI in the area of the right bank upstream of Wubao had the strongest correlation with precipitation, and the correlation coefficient reached 0.5312, indicating that the vegetation NDVI in this area was significantly affected by precipitation. In addition, the spatial correlation between vegetation NDVI and precipitation in the areas of the right bank downstream of Wubao and the left bank of Hekou town to Longmen was also relatively strong, whereas the correlation in the trunk stream area of Longmen to Sanmen Gorge was the weakest, with a correlation coefficient of 0.0003, indicating that the vegetation NDVI in this area was less affected by precipitation than in other areas.

Fig. 19 shows that in the past 30 years, the areas with a positive correlation coefficient between vegetation NDVI and sunshine duration accounted for 37.57% of the total area and were mainly distributed in the middle and upper areas of Shanxi–Shaanxi Gorge, and the areas with a negative correlation coefficient accounted for 62.43% of the total area and were mainly distributed in the southwest and south parts. The areas with an extremely positive or positive correlation between vegetation NDVI and sunshine duration accounted for approximately 2.68% of the study area and were mainly distributed in the areas of Hohhot, Yinchuan, and Yulin. The areas with an extremely negative or negative correlation between vegetation NDVI and sunshine duration accounted for approximately 17.85% of the study area and were mainly distributed in the areas of Maqu, Xining, Hezuo, and the Wei River. Overall, in the upper and middle reaches of the Yellow River, the vegetation NDVI in the southern part had a negative correlation with sunshine duration, whereas the correlation in other regions was not significant. Focusing on each tributary area, vegetation NDVI in the area of Sanmenxia–Xiaolangdi had the strongest correlation with sunshine duration, the correlation coefficient reaching 0.433, indicating that the vegetation NDVI in this area was more significantly affected by sunshine duration, whereas the correlation between vegetation NDVI and sunshine duration was the weakest in the endorheic basins (correlation coefficient 0.0235), indicating that the vegetation NDVI in this area was less affected by sunshine duration.

IV. Discussion

Spatiotemporal changes in vegetation can cause changes in land surface parameters [4], [44]. Currently, monitoring long-term vegetation changes and analyzing the influencing factors have become important parts of the research on global changes [45]. Since the 1980s, the combination of natural evolution and intense human activities have caused significant changes in the pattern of resources and the environment in the Yellow River Basin, which have further affected the plans for development and utilization and have caused many environmental degradation and ecological destruction problems [46]. It is urgent to systematically and scientifically study the change characteristics in the pattern of watershed ecology and the human settlements, identify major ecological environmental problems, and put forward solutions in order to provide a decision-making basis for the sustainable development of the Yellow River Basin. The conclusions of this study are consistent with existing results [47]–[51]. Specifically, this study concludes that vegetation NDVI in the growing seasons of the Yellow River Basin exhibited an overall rising trend with fluctuations. In terms of spatial distribution, vegetation NDVI had strong regional differences, showing an overall zonal distribution decreasing from southeast to northwest. Other studies also have shown that vegetation NDVI is more sensitive to human activities in relatively dry areas [52], and improvements in agricultural management (especially irrigated agriculture) and the implementation of vegetation construction projects (such as returning farmland to forests) can effectively increase vegetation cover at a local or even a regional scale [53].

In fact, the response of vegetation NDVI to natural evolution and human activities in different areas is quite complex, and there is a lack of comprehensive and systematic studies on the response relationship between the two [8], [54]. This study also has its shortcomings. The period covered by the RS time-series data is relatively long, and the spatial resolutions of the MODIS and GIMMS NDVI datasets are inconsistent, so the resolution of the MODIS data was resampled to 8 km using a resampling tool. After the resampling, the spatial resolution was low, so it was impossible to conduct a detailed study on vegetation types. In addition, this study only analyzed the effects of temperature, precipitation, and sunshine duration on the vegetation NDVI. Because of the lack of relevant information, the impacts of other climatic and topographic factors, such as evaporation, wind speed, and humidity, and human activities were not analyzed. In the future, quantitative studies with high-resolution data and comprehensive inclusion of factors should be conducted on the response of vegetation to human activities, in order to systematically study this response mechanism.

V. Conclusion

In the past 30 years, the annual mean vegetation NDVI in the middle and upper reaches of the Yellow River grew by approximately 31.28%. The NDVI change in 81.83% of the pixels was positive, i.e., vegetation showed an increasing trend in them, and the highest vegetation change rate reached 0.025. The NDVI change in 18.17% pixels was negative, i.e., vegetation showed a decreasing trend in them. The distribution of temperature exhibited a pattern of low in the southwest and high in the southeast, showing an obvious rising trend. The distribution of precipitation showed a gradual decrease from southeast to northwest, exhibiting a gradual upward trend. The distribution of sunshine duration showed a gradual increase from southeast to northwest, exhibiting a significant decreasing trend. From the perspective of the NDVI change trend, the vegetation status in the study area has been significantly improved in the past 30 years. Arid, semiarid, and subhumid areas have a significant increase, but not a significant decrease, which is mainly concentrated in the semihumid area of the source area of the Yellow River, which is related to frequent human activities.

Over the past 30 years, the vegetation growth in the upper and middle reaches of the Yellow River is driven by precipitation, temperature, and sunshine hours, and most areas are positively correlated. The sunshine hours have a more obvious impact on NDVI. Especially in arid areas, NDVI has the closest relationship with sunshine. The correlation between precipitation is the worst in the subhumid zone and the best in the semiarid zone, whereas the correlation between NDVI and temperature is the highest in the subhumid zone and the lowest in the arid zone. The annual mean NDVI showed a positive correlation with temperature, and the correlation coefficient showed a gradual increasing trend from northeast to southwest. The areas with a positive correlation accounted for 81.15% of the study area, and the areas with a negative correlation accounted for 18.85%. The latter were distributed in the northeastern part of the study area (the north bank of Hekou town) and the area of Lanzhou to Xiaheyan. The annual mean NDVI and precipitation had a correlation coefficient of 0.708, and this coefficient exhibited a gradual increasing trend from southwest to northeast. The areas with a positive correlation coefficient accounted for 79.11% and were mainly distributed in the middle reach of the Yellow River. The areas with a negative correlation coefficient accounted for 20.89% and were mainly distributed in the southwestern part of the study area and the area along the Wei River. The correlation between the annual mean NDVI and sunshine duration was –0.510. The areas with a positive correlation coefficient accounted for 37.57% and were mainly distributed in the middle and upper areas of Shanxi–Shaanxi Gorge. The areas with a negative correlation accounted for 62.43% and were mainly distributed in the southwest and south parts of the study area.

References

[1] R. Costanza *et al.*, "The value of the world's ecosystem services and natural capital," *Nature*, vol. 387, pp. 253–260, May 1997.

[2] J. Y. Fang *et al.*, "Vegetation-climate relationship and its application in the division of vegetation zone in China," *Acta Botanica Sin.*, vol. 44, no. 9, pp. 1105–1122, Sep. 2002.

[3] S. Piao *et al.*, "Effect of climate and CO_2 changes on the greening of the Northern Hemisphere over the past two decades," *Geophys. Res. Lett.*, vol. 33, no. 23, Dec. 2006, Art. no. L23402.

[4] D. Kong *et al.*, "Seasonal vegetation response to climate change in the northern hemisphere (1982-2013)," *Global Planet. Change*, vol. 148, pp. 1–8, Jan. 2017.

[5] L. Liang *et al.*, "Influence of different bandwidths on LAI estimation using vegetation indices," *IEEE J. Sel. Topics Appl. Earth Observ. Remote Sens.*, vol. 13, pp. 1494–1502, Apr. 2020, doi: 10.1109/JSTARS.2020.2984608.

[6] J. Yang *et al.*, "Influence of urban morphological characteristics on thermal environment," *Sustain. Cities Soc.*, vol. 72, 2021, Art. no. 103045.
[7] Y. Liu *et al.*, "Spatial and temporal patterns of global NDVI trends: Correlations with climate and human factors," *Remote Sens.*, vol. 7, no. 10, pp. 13233–13250, Oct. 2015.
[8] X. M. Yang *et al.*, "Vegetation variation in the North Hemisphere under climate warming in the last 30 years," *Arid Zone Res.*, vol. 33, no. 2, pp. 379–391, Mar. 2016.
[9] R. B. Myneni, F. G. Hall, P. J. Sellers, and A. L. Marshak, "The interpretation of spectral vegetation indexes," *IEEE Trans. Geosci. Remote Sens.*, vol. 33, no. 2, pp. 481–486, Mar. 1995.
[10] W. Lucht *et al.*, "Climatic control of the high-latitude vegetation greening trend and Pinatubo effect," *Science*, vol. 296, no. 31, pp. 1687–1689, May. 2002.
[11] J. Wang, J. J. Meng, and Y. L. Cai, "Assessing vegetation dynamics impacted by climate change in the southwestern Karst region of China with AVHRR NDVI and AVHRR NPP time-series," *Environ. Geol.*, vol. 54, no. 6, pp. 1185–1195, Jul. 2008.
[12] Y. Zhang *et al.*, "Seasonal and interannual changes in vegetation activity of tropical forests in Southeast Asia," *Agricultural Forest Meteorol.*, vol. 244, pp. 1–10, Aug. 2016.
[13] H. Ye *et al.*, "Spatio-temporal characteristics of evapotranspiration and its relationship with climate factors in the source region of the Yellow River from 2000 to 2014," *Acta Geographica Sin.*, vol. 73, no. 11, pp. 2117–2134, Nov. 2018.
[14] C. Wang, J. Chen, Y. Tang, T. A. Black, and K. Zhu, "A novel method for removing snow melting-induced fluctuation in GIMMS NDVI3g data for vegetation phenology monitoring: A case study in deciduous forests of North America," *IEEE J. Sel. Topics Appl. Earth Observ. Remote Sens.*, vol. 11, no. 3, pp. 800–807, Mar. 2018.
[15] Y. F. Wang and J. L. Jing, "Spatial-temporal variations of vegetation cover and its response to climate factors in Guangxi over past 15 years," *Res. Agricultural Modernization*, vol. 38, no. 6, pp. 1086–1096, Jun. 2017.
[16] X. Y. Li, Z. Y. Ren, and C. Zhang, "The correlation analysis and space-time changes of NDVI and hydro-thermal index in Hanjiang Basin," *Geographical Res.*, vol. 32, no. 9, pp. 1623–1633, Sep. 2013.
[17] Z. Y. Xu *et al.*, "Trends in global vegetative drought from long-term satellite remote sensing data," *IEEE J. Sel. Topics Appl. Earth Observ. Remote Sens.*, vol. 13, pp. 815–826, Feb. 2020, doi: 10.1109/JSTARS.2020.2972574.
[18] K. Jin, F. Wang, and P. Li, "Responses of vegetation cover to environmental change in large cities of China," *Sustainability*, vol. 10, no. 1, Feb. 2018, Art. no. 270.
[19] C. Tucker *et al.*, "An extended AVHRR 8-km NDVI dataset compatible with MODIS and SPOT vegetation NDVI data," *Int. J. Remote Sens.*, vol. 26, pp. 4485–4498, Mar. 2005.
[20] F. Y. Cheng *et al.*, "The dynamics and main driving factors of coastal vegetation in Guangxi based on MODIS NDVI," *Acta Ecologica Sin.*, vol. 37, no. 3, pp. 788–797, Mar. 2017.
[21] K. Jin *et al.*, "Contribution of climatic change and human activities to vegetation NDVI change over China during 1982-2015," *Acta Geographica Sin.*, vol. 75, no. 5, pp. 961–974, May 2020.
[22] J. R. Eastman *et al.*, "Global trends in seasonality of normalized difference vegetation index (NDVI), 1982-2011," *Remote Sens.*, vol. 5, no. 10, pp. 4799–4818, Sep. 2013.
[23] S. L. Piao *et al.*, "Changes in satellite-derived vegetation growth trend in temperate and boreal Eurasia from 1982 to 2006," *Global Change Biol.*, vol. 17, no. 10, pp. 3228–3239, Mar. 2011.
[24] S. S. Peng *et al.*, "Recent change of vegetation growth trend in China," *Environ. Res. Lett.*, vol. 6, no. 4, pp. 44027–44029, Dec. 2011.
[25] D. J. Jiang *et al.*, "Interannual variability and correlation of vegetation cover and precipitation in eastern China," *Theor. Appl. Climatol.*, vol. 118, pp. 93–105, Nov. 2014.
[26] X. L. Wang and X. Y. Hou, "Variation of normalized difference vegetation index and its response to extreme climate in coastal China during 1982-2014," *Geographical Res.*, vol. 38, no. 4, pp. 807–821, Apr. 2019.
[27] J. M. Paruelo and W. K. Lauenroth, "Regional patterns of normalized difference vegetation index in North American scrublands and grasslands," *Ecology*, vol. 76, pp. 1888–1898, Sep. 1995.
[28] L. Milich and E. Weiss, "GAC NDVI images: Relationship to rainfall and potential evaporation in the grazing lands of The Gourma (Northern Sahel) and in the croplands of the Niger-Nigeria border (Southern Sahel)," *Int. J. Remote Sens.*, vol. 21, no. 2, pp. 261–280, Nov. 2010.
[29] K. Ichii, A. Kawabata, and Y. Yamaguchi, "Global decadal changes in NDVI and its relationships to climate variables," *Int. J. Remote Sens.*, vol. 22, no. 7, pp. 1377–1382, Nov. 2010.
[30] M. Lamchin *et al.*, "Long-term trend and correlation between vegetation greenness and climate variables in Asia based on satellite data." *Sci. Total Environ.*, vol. 618, pp. 1089–1095, Oct. 2017.
[31] Y. Richard and I. Poccard, "A statistical study of NDVI sensitivity to seasonal and international rainfall variation in southern Africa," *Int. J. Remote Sens.*, vol. 19, pp. 2907–2920, Oct. 1998.
[32] R. Suzuki, T. Nomaki, and T. Yasunari, "Spatial distribution and its seasonality of satellite-derived vegetation index (NDVI) and climate in Siberia," *Int. J. Climatol.*, vol. 21, no. 11, pp. 1321–1335, Sep. 2001.
[33] H. Y. Sun *et al.*, "Analysis of the vegetation cover change and the relationship between NDVI and environmental factors by using NOAA time series data," *J. Remote Sens.*, vol. 2, no. 3, pp. 204–210, Mar. 1998.
[34] J. Liu, Z. M. Wen, and C. C. Gang, "Normalized difference vegetation index of different vegetation cover types and its responses to climate change in the Loess Plateau," *Acta Ecologica Sin.*, vol. 40, no. 2, pp. 678–691, Fab. 2020.
[35] L. Zhou *et al.*, "Variations in northern vegetation activity inferred from satellite data of vegetation index during 1981 to 1999," *J. Geophys. Res., Atmos.*, vol. 106, no. D17, pp. 20069–20083, Sep. 2001.
[36] W. Sun *et al.*, "Spatiotemporal vegetation cover variations associated with climate change and ecological restoration in the Loess Plateau," *Agricultural Forest Meteorol.*, vols. 209/210, no. 1, pp. 87–99, Sep. 2015.
[37] J. P. Xi, "Speech at a symposium on ecological protection and quality development in the Yellow River Basin," *Qiushi*, vol. 20, pp. 1–5, Sep. 2019.
[38] Z. Y. Zheng, M. X. Lu, and Z. G. Ma, "Climate, hydrology, and vegetation coverage changes in source region of Yellow River and countermeasures for challenges," *Bull. Chin. Acad. Sci.*, vol. 35, no. 1, pp. 61–72, Jun. 2020.
[39] L. Ye *et al.*, "Climate change in the upper Yellow River Basin and its impact on ecological vegetation and runoff from 1980 to 2018," *Trans. Atmos. Sci.*, vol. 43, no. 6, pp. 967–979, Nov. 2020.
[40] B. P. Ren and Q. Zhang, "The strategic design and supporting system construction of high-quality development in the Yellow River Basin," *Reform*, vol. 308, no. 10, pp. 26–34, Oct. 2019.
[41] J. Gu *et al.*, "Effects of NDVI/land-use on spatiotemporal changes of evapotranspiration in the Yellow River Basin," *Arid Land Geography*, vol. 44, no. 1, pp. 158–167, 2021.
[42] J. P. Yang, Y. J. Ding, and R. S. Chen, "Preliminary study on eco-environmental vulnerability assessment of the source region of the Yangtze River and Yellow River," *J. Desert Res.*, vol. 27, no. 6, pp. 1012–1017, Nov. 2007.
[43] B. Dong, Z. K. Feng, and G. Y. Qian, "Dynamic study on land use and forest land transfer based on remote sensing in Yellow River Basin of Shandong Province, China," *J. Fujian Agriculture Forestry Univ. (Natural Sci.)*, vol. 39, no. 6, pp. 646–650, Jun. 2010.
[44] R. N. Guo *et al.*, "Analysis of the factors affecting the spatiotemporal soil moisture distribution based on the temperature-vegetation drought index," *J. Irrigation Drainage*, vol. 37, no. 4, pp. 52–58, Apr. 2018.
[45] K. Jin *et al.*, "Impacts of climate change and human activities on vegetation NDVI in China from 1982 to 2015," *Acta Geographica Sin.*, vol. 75, no. 5, pp. 961–974, May 2020.
[46] Y. Wang *et al.*, "Analysis on the change of resources and environment patterns of the Yellow River Basin in the past 40 years and suggestions for geological survey," *Geol. China*, vol. 48, no. 1, pp.1–20, Oct. 2020.
[47] R. Q. Yuan and S. Qing, "Response of the normalized difference vegetation index to water storage in terrestrial basin of the Yellow River Basin: Taking 2002-2015 as an example," *J. Irrigation Drainage*, vol. 39, no. 10, pp. 115–122, Oct. 2020.
[48] L. L. Liu and H. M. Xu, "The law of NDVI change of main vegetation types in the Yellow River Basin and its relationship with meteorological factors," *Chin. J. Agricultural Meteorol.*, vol. 28, no. 3, pp. 334–337, Jun. 2007.
[49] H. He *et al.*, "Variation characteristics of normalized vegetation index (NDVI) and its response to climate change in northern China from 1982 to 2015," *J. Ecol. Rural Environ.*, vol. 36, no. 1, pp. 70–80, Jan. 2020.
[50] J. Yang *et al.*, "Contribution of urban ventilation to the thermal environment and urban energy demand: Different climate background perspectives," *Sci. Total Environ.*, vol. 795, Nov. 2021, Art. no. 148791.
[51] X. Luo *et al.*, "Suitability of human settlements in mountainous areas from the perspective of ventilation: A case study of the main urban area of Chongqing," *J. Cleaner Prod.*, vol. 310, Aug. 2021, Art. no. 127467.
[52] J. Bai *et al.*, "Satellite-observed vegetation stability in response to changes in climate and total water storage in central Asia," *Sci. Total Environ.*, vol. 659, pp. 862–871, Apr. 2019.

[53] Z. B. Xin, J. X. Xu, and W. Zheng, "Spatiotemporal variations of vegetation cover on the Chinese Loess Plateau (1981–2006): Impacts of climate changes and human activities," *Sci. China Ser. D, Earth Sci.*, vol. 51, no. 1, pp. 67–78, Jan. 2008.
[54] J. J. Li, "Analysis of NDVI spatio-temporal changes and driving forces in the eight provinces of western China in the past 30 years," China Univ. Mining Technol., Beijing, China, 2019.

Chengpeng Lu (Member, IEEE) received the B.S. degree in resource environment and urban and rural planning management and Ph.D. degree in human geography from Lanzhou University (LZU), Lanzhou, China, in 2007 and 2013, respectively.

He is currently a Professor with the Institute of County Economic Development and Rural Revitalization Strategy, LZU. His research interests include man-land relationship, regional ecology, population, resource and environmental economics, and adapting climate change.

Muchen Hou received the B.E. degree in thermal and power engineering from Chongqing University, Chongqing, China, in 2019. He is currently working toward the master's degree in applied economics with the Faculty of Economics, Lanzhou University, Lanzhou, China.

His research interests include population, resource, and environmental economics.

Zhiliang Liu received the B.B.A. degree in management from Henan University of Economics and Law, Zhengzhou, China, in 2018. He is currently working toward the master's degree in applied economics with the Faculty of Economics, Lanzhou University, Lanzhou, China.

His research interests include population, resource, and environmental economics.

Hengji Li received the M.S. degree in human geography from Lanzhou University, Lanzhou, China, in 2007.

He is currently an Assistant Researcher with the Northwest Institute of Eco-Environment and Resources, Chinese Academy of Sciences, Lanzhou, China. His research interests include regional sustainable development and regional carbon emission.

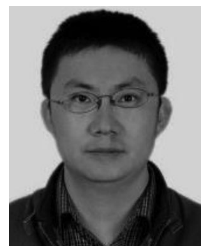

Chenyu Lu received the B.S. degree in geographic information system and Ph.D. degree in human geography from Lanzhou University, Lanzhou, China, in 2004 and 2009, respectively.

He is currently an Associate Professor with the Northwest Normal University, Lanzhou. His research interests include interactions analysis on human-environmental system and regional sustainability, based on the techniques of GIS and employing the transdisciplinary and interdisciplinary approaches.